Short cracks in knee meniscus tissue cause strain concentrations, but not weakness, in single-cycle uniaxial tension

John M. Peloquin[1,*], Michael H. Santare[2], and Dawn M. Elliott[1]

[1]Department of Biomedical Engineering, University of Delaware, Newark, DE, USA
[2]Department of Mechanical Engineering, University of Delaware, Newark, DE, USA
[*]Corresponding author

March 30, 2018

Abstract

Tears are central to knee meniscus pathology. From a mechanical perspective, meniscus tears are a type of crack-like defect. In many materials, cracks create stress concentrations that cause failure by fracture and thereby reduce the material's effective strength. It is currently unknown whether the meniscus is vulnerable to fracture. If meniscus tears cause fracture, this would have significant repercussions for management of meniscus pathology. The objective of this study was to determine if short crack-like defects in the meniscus, representing short meniscus tears, cause fracture and, by unloading the cut region, stress concentrations. Failure stress was compared between cracked and control specimens to determine if fracture occurred. Strain concentrations near the crack tip were quantified using digital image correlation (DIC) and used as an indicator of stress concentrations. The presence of cracks did not affect the meniscus' failure stress (effect < 0.86 s.d.; $\beta = 0.2$), and cracks almost always became blunt or were deflected along fascicle boundaries instead of growing. However, significant strain concentrations were observed near the crack tip even at low applied stress. Although the maintenance of macroscopic failure stress indicates low risk of failure for short meniscus tears, long-term crack growth and failure, such as by accumulation of tissue or cell damage, may still occur due to the strain concentrations.

1 Introduction

Tears are the most common pathology to afflict the knee meniscus. Their direct symptoms include pain, mechanical deficiency, and increased risk of osteoarthritis (Englund et al. 2012; Øiestad et al. 2009; Cohen et al. 2007; Englund et al. 2008). Meniscus tears can also cause serious secondary harm, as the most straightforward treatment for a tear—partial

or total meniscectomy—further increases the risk of osteoarthritis (Magnussen et al. 2009; Shelbourne and Gray 2000; Feucht et al. 2015; Anetzberger et al. 2014; Petty and Lubowitz 2011) and repair of a torn meniscus, especially when the tear is in the inner avascular region, is not always feasible (Arnoczky and Warren 1983; Englund et al. 2012). Meniscus tears may occur suddenly, suggestive of immediate failure from a single overload event (Fink et al. 2018; Greis et al. 2002; Wagemakers et al. 2008; Cox et al. 2009; Lento and Akuthota 2000; Poulsen and Johnson 2011; Paul et al. 2003), but are also known to grow over time in vivo (Kumm et al. 2015; Khan et al. 2016). Although short (< 5–10 mm) tears often do not merit immediate clinical concern (Lento and Akuthota 2000; Stärke et al. 2009; Roeddecker et al. 1994; Lento and Akuthota 2000; Seil et al. 2009), they have the potential to grow and become more serious with time. To aid efforts to prevent and repair meniscus tears, it is important to understand the mechanics of how they form and grow.

From a mechanical perspective, a meniscus tear is a flaw or crack-like defect, subsequently referred to simply as a crack. A crack in a material, in principle, causes a stress concentration and may make it vulnerable to failure by fracture. In fracture, failure occurs by crack growth, and the peak stress is determined by the crack geometry (which determines the strength of the stress concentration) and the material's fracture toughness. In contrast, in the absence of fracture (as in an intact, or crack-free, material) the material fails as a whole by bulk rupture. In this case the peak stress is equal to the material's strength. For any given circumstance, the failure mode requiring the least peak stress prevails and determines when the material fails. Prediction of the fate of a torn meniscus requires that both fracture and bulk rupture be considered as possible failure modes.

The circumstances under which the meniscus may fail by fracture are ambiguous. Fracture occurs by crack growth, and meniscus tears (i.e., cracks) grow in vivo (Kumm et al. 2015; Khan et al. 2016). This suggests fracture may occur in the meniscus. Data from mechanical tests of other tissues that are similar to meniscus fibrocartilage, namely superficial zone articular cartilage (Chin-Purcell and Lewis 1996) and temporomandibular joint disc (Koombua et al. 2006), indicate that fracture probably occurs in those tissues (Taylor et al. 2012). However, cracks in tendon tend to blunt instead of propagating (Schechtman and Bader 1997; Von Forell and Bowden 2014b; Von Forell and Bowden 2014a; Andarawis-Puri et al. 2009; Locke et al. 2017; Szczesny et al. 2015). A definitive test to determine if a cracked specimen failed by fracture is to check if its peak stress was less than that of identically tested crack-free specimens (Taylor et al. 2012). This foundational work to determine whether the meniscus is vulnerable to fracture has not yet been done. It is therefore unknown whether meniscus tissue fails by fracture or bulk rupture, and the peak stress of a torn meniscus cannot be predicted with confidence.

Even if a crack does not cause fracture, the stress concentration it creates may cause local overload and tissue or cell damage. Local damage may be an important mediator of long-term meniscus degeneration and tear growth by processes such as fatigue. Tissue near the tip of a naturally occurring meniscus tear takes less energy to rupture than tissue in a crack-free contralateral control meniscus (Roeddecker et al. 1994), suggesting that natural tears create zones of weak, damaged tissue near their tips. However, the size, shape, and magnitude of crack-associated stress and strain concentrations in meniscus are unknown. Development of a stress concentration at a crack tip typically occurs by a shift in load distribution, relative to an intact specimen, from the region cut by the crack to the intact region. The degree of unloading in the cut region is therefore mechanistically important, but is sim-

ilarly unknown. At the present time, the magnitude of near-tip stress–strain concentrations and cut region unloading cannot be accurately predicted due to incomplete knowledge of the meniscus' mechanical properties. Experiments are needed to show how a crack affects the meniscus' strain fields and permit inference of its stress fields.

The objectives of this study were to determine (a) whether short cracks in meniscus tissue, representing short meniscus tears, cause failure by fracture or bulk rupture, (b) whether they create strain concentrations near their tips, and (c) whether they cause the region they cut to become unloaded. To test whether the meniscus fails by fracture, peak stress was compared between cracked and crack-free specimens (Taylor et al. 2012). Meniscus tissue specimens were tested in both circumferential and radial uniaxial tension so as to examine both fiber and matrix rupture phenomena. Edge cracks were used because they are a standard fracture test scenario (single edge notch tension). Circumferential tension specimens with angled center cracks were also tested because prior FEA suggested this loading scenario produces a greater stress concentration and a higher risk of fracture (Peloquin and Elliott 2016). Together, these test scenarios measure mechanical behavior relevant to radial, oblique, and circumferential vertical meniscus tears, which are more closely associated with overload and trauma than aging and degeneration (Lento and Akuthota 2000; Oberlander and Pryde 1994; Hardin et al. 1992). To test whether near-tip strain concentrations are present, and to measure their magnitude, strain fields were measured using digital image correlation (DIC) and strain in cracked specimens was compared between near-tip and away-from-tip regions. Similarly, to test whether the cut region in cracked specimens is unloaded, strain was compared between cut and intact regions. Rupture morphology was also recorded to facilitate comparison with other work. Results are discussed in terms of their significance with respect to whole-meniscus damage and failure in vivo.

2 Methods

2.1 Specimen preparation

Specimens were prepared for three test groups—circumferential tension with a 90° edge crack, circumferential tension with a 45° center crack, and radial tension with a 90° edge crack—with corresponding circumferential and radial tension crack-free control groups (Figure 1). As established by prior work (Peloquin et al. 2016), circumferential specimens were cut with expanded grip regions to facilitate fiber loading. The specimens were prepared from adult (age > 30 months) bovine menisci.

Menisci (mixed lateral & medial) were purchased from Animal Technologies, Inc. (Tyler, TX) and stored frozen (−20 °C). One specimen per meniscus was prepared using a Leica SM2400 sledge microtome (with a freezing stage) to plane the meniscus to a target thickness of 1.0–1.5 mm, with the specimen plane normal to the proximal–distal axis. The specimen was then trimmed to its final in-plane dimensions, its cross-sectional area measured by scanning across its width with a laser displacement sensor (Szczesny et al. 2012; Favata 2006), and its surface airbrushed with Verhoeff's stain to facilitate digital image correlation from test video. Each edge crack was cut with a fresh #11 scalpel blade to a target length of 3 mm. Each center crack was cut with a razor blade broken to the target crack length of 3 mm. Measured specimen dimensions are reported in Table 1. Except when the

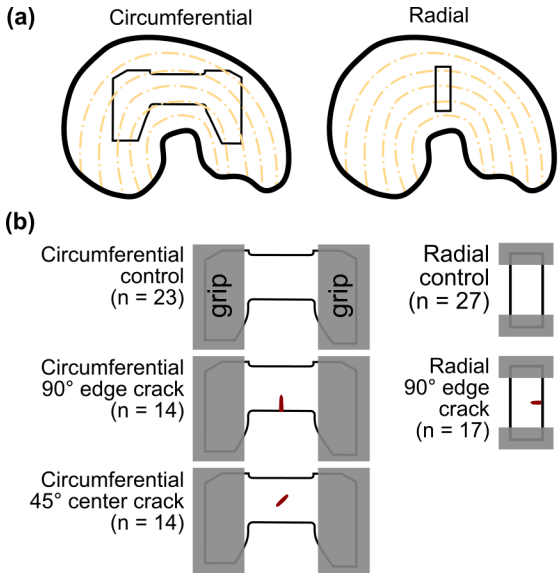

Figure 1: Specimen schematics. (a) Site of specimen dissection. (b) Specimen shapes for each of the analysis groups (circumferential 90° edge crack, circumferential 45° center crack, and radial 90° center crack) and their crack-free controls.

specimens were being actively manipulated, they were kept covered under PBS-dampened gauze to minimize dehydration.

Table 1: Specimen dimensions (mean ± sd).

Group	Width (mm)	Grip-to-grip length (mm)	Thickness (mm)	Crack length (mm)
Circumferential control	8.0 ± 2.1	16.2 ± 2.3	1.2 ± 0.2	
Circumferential 90° edge crack	9.2 ± 2.4	16.5 ± 1.9	1.0 ± 0.2	2.9 ± 0.4
Circumferential 45° center crack	9.8 ± 2.0	16.0 ± 2.1	1.2 ± 0.3	3.1 ± 0.3
Radial control	5.6 ± 1.0	8.1 ± 1.6	1.5 ± 0.3	
Radial 90° edge crack	5.9 ± 1.6	8.1 ± 1.8	1.5 ± 0.3	2.0 ± 0.4

2.2 Tensile test protocol

Tensile testing was done following the same procedure as in Peloquin et al. (2016). The tensile test protocol consisted of (a) 20 kPa preload, which was used to establish the specimen's undeformed reference length, (b) 10 cycles of preconditioning to 4% grip-to-grip strain, and (c) stretch to failure. The displacement rate was 0.5 mm/s (i.e., quasi-static). Video was recorded during the test at 15 fps and 1392 × 1000 px. The image scale was ~ 40 px/mm for circumferential specimens and ~ 60 px/mm for radial specimens.

Tested specimens were classified according to published definitions as terminating in midsubstance rupture, mixed rupture, grip line rupture, gripped region failure, or no rupture

(Peloquin et al. 2016). Tests terminating in longitudinal split, gripped region failure, or no rupture were excluded from all analysis because mean stress at the failure site cannot be accurately calculated for these failure types. The counts of each type of rupture are presented in Table 2. The counts of tests used for analysis are given by group in Figure 1b.

Table 2: Counts for each type of rupture by specimen group.

Group	Rupture Type	Included in analysis	Control	90° edge crack	45° center crack
Circumferential	Midsubstance rupture	Yes	5	2	4
	Mixed rupture	Yes	11	12	8
	Grip line rupture	Yes	7	0	2
	Gripped region failure	No	8	6	5
	Longitudinal split	No	0	2	0
	No rupture	No	5	0	2
Radial	Midsubstance rupture	Yes	9	11	
	Mixed rupture	Yes	3	3	
	Grip line rupture	Yes	15	3	
	Gripped region failure	No	0	1	
	Longitudinal split	No	0	0	
	No rupture	No	1	2	

2.3 Stress and strain data processing

The tensile tests' stress–strain curves were summarized using peak stress σ_{peak} and strain, tangent modulus (measured at the yield point), and yield stress and strain. Strain was calculated continuously using the current grip-to-grip length l and the initial grip-to-grip length l_0 and reported as stretch ratio ($\lambda = l/l_0$) or Lagrange strain ($E_{xx} = 1/2[\lambda^2 - 1]$). The yield point was identified as the inflection point in the stress–strain curve as in Peloquin et al. (2016). For cracked specimens, the intact cross-sectional area (thickness × (total width − crack length along y-axis)) was used for stress calculations.

Lagrange strain fields were computed across the specimen surface from the video recordings using 2D digital image correlation (Vic-2D 2009; Correlated Solutions, Columbia, SC). Three strain components were analyzed: longitudinal strain (grip-to-grip direction; E_{xx}), transverse strain (E_{yy}), and shear strain magnitude ($|E_{xy}|$). The correlation window (subset size) was 0.7 × 0.7 mm, and exhaustive search, low pass filtering, and incremental correlation were enabled. Post-processing used a 15 px exponential decay filter. Trial runs during study development showed that only the subset size setting had a strong influence on the calculated strain field. The choice of 0.7 × 0.7 mm subset size was a compromise between the needs of (a) minimizing spurious correlations, which favors a large correlation window, and (b) retaining spatial resolution to identify strain concentrations and interfascicle sliding, which favors a small correlation window.

Quantitative analysis of strain fields was done by comparison of strain statistics between regions of interest (ROIs). To test for the existence of strain concentrations near the crack tip, the DIC strain field was partitioned into near-tip and away-from-tip ROIs (Figure 4a). The ROI size was chosen to be of similar size to the strain concentrations visible in the strain field images. The near-tip ROIs for analysis of E_{xx} extended, relative to the crack tip,

+0.7 mm in the crack pointing direction and ±0.7 mm in the loading direction. The near-tip ROIs for analysis of E_{yy} and E_{xy} were defined to extend +0.7 mm in the crack pointing direction and, because the E_{yy} and E_{xy} strain fields were elongated in the loading direction, ±1.05 mm in the loading direction. To test for differences in strain between tissue cut and not cut by a crack, cut and intact ROIs were also defined (Figure 6a). Comparisons of DIC strain statistics between paired (a) near-tip and away-from-tip and (b) cut and intact ROIs were made at stress levels from $0.25\sigma_{peak}$ to $0.9\sigma_{peak}$ for circumferential specimens and, due to loss of DIC tracking at high strain for several radial specimens, $0.25\sigma_{peak}$ to $0.7\sigma_{peak}$ for radial specimens.

2.4 Statistics and inference

The hypothesis that cracks weaken the meniscus was tested using unpaired Welch t-tests to compare peak stress (σ_{peak}) between cracked and control specimens for each of the three test cases (circumferential tension 90° edge cracks, circumferential tension 45° center cracks, and radial tension 90° edge cracks). Since this hypothesis was specifically that cracked σ_{peak} < control σ_{peak}, peak stress was compared using a one-sided t-test. The other stress–strain parameters did not have a specific hypothesized direction of change and so were compared between cracked and control specimens with two-sided t-tests. The type I error rate for all statistical tests was set to 0.05.

The hypothesis that cracks generate strain concentrations near their tips was tested by comparing DIC strain in the near-tip region to the away-from-tip region (Figure 4a). Similarly, the hypothesis that cracks reduce strain in the region they cut was tested by comparing DIC strain in the cut region to the intact region (Figure 6a). Comparisons between DIC strain in each ROI were done using the mean strain in each region by paired (within-specimen comparison) Wilcoxon tests, due to skewed and very heavy-tailed distributions.

The hypothesis that cracks propagate in meniscus tissue was tested by qualitative evaluation. If incremental crack propagation had occurred, measurement of changes in crack length over time would have been warranted, but, as is evident in Section 3.3, qualitative description was more appropriate to record the tissue's actual behavior.

The underlying data for all results is available, hosted on the Open Science Framework, under a CC-BY license (doi: 10.17605/osf.io/hqxt8).

3 Results

3.1 Effect of cracks on stress–strain curve parameters

Whether or not fracture occurred was determined by comparing peak stress for each group of cracked specimens with its corresponding control group (Figure 2). None of the crack groups (circumferential 90° edge crack, circumferential 45° center crack, and radial 90° edge crack; Figure 1) had peak stress significantly less than their corresponding controls ($p > 0.2$ for all). The study had power = 0.8 to detect a 0.86 s.d. decrease in circumferential peak stress or a 0.78 s.d. decrease in radial peak stress, so this negative result indicates that no meaningful difference exists. Therefore the specimens most likely failed by bulk rupture.

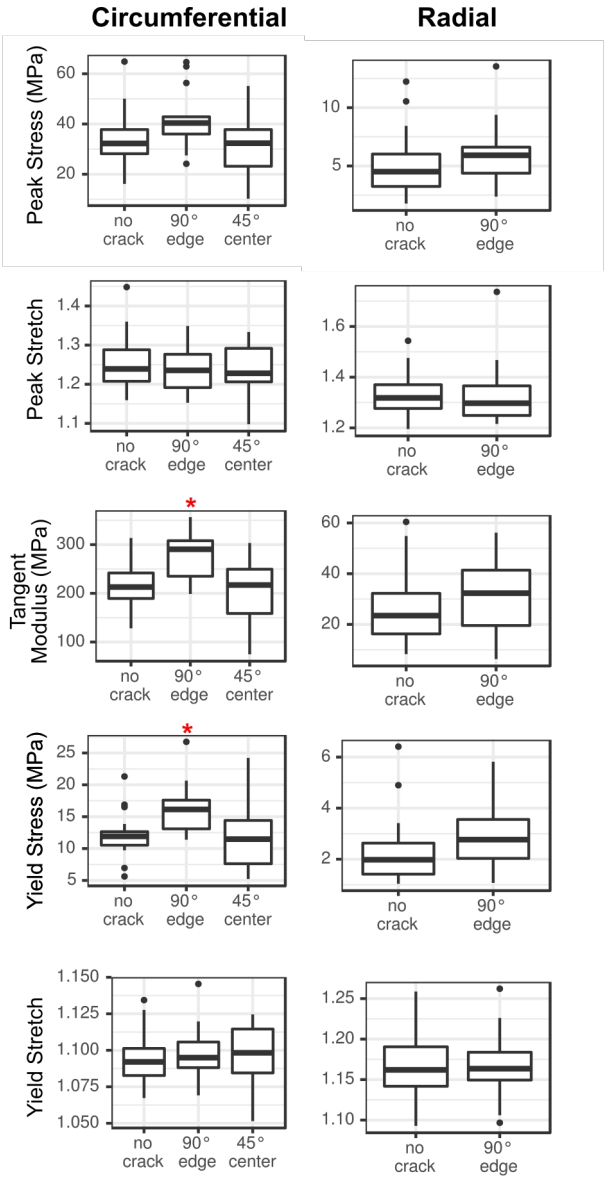

Figure 2: Comparison of stress–strain curve parameters between cracked specimens and their corresponding controls. The boxplots are in Tukey's style. * indicates cracked $\neq$ control, Welch t-test, $p < 0.05$.

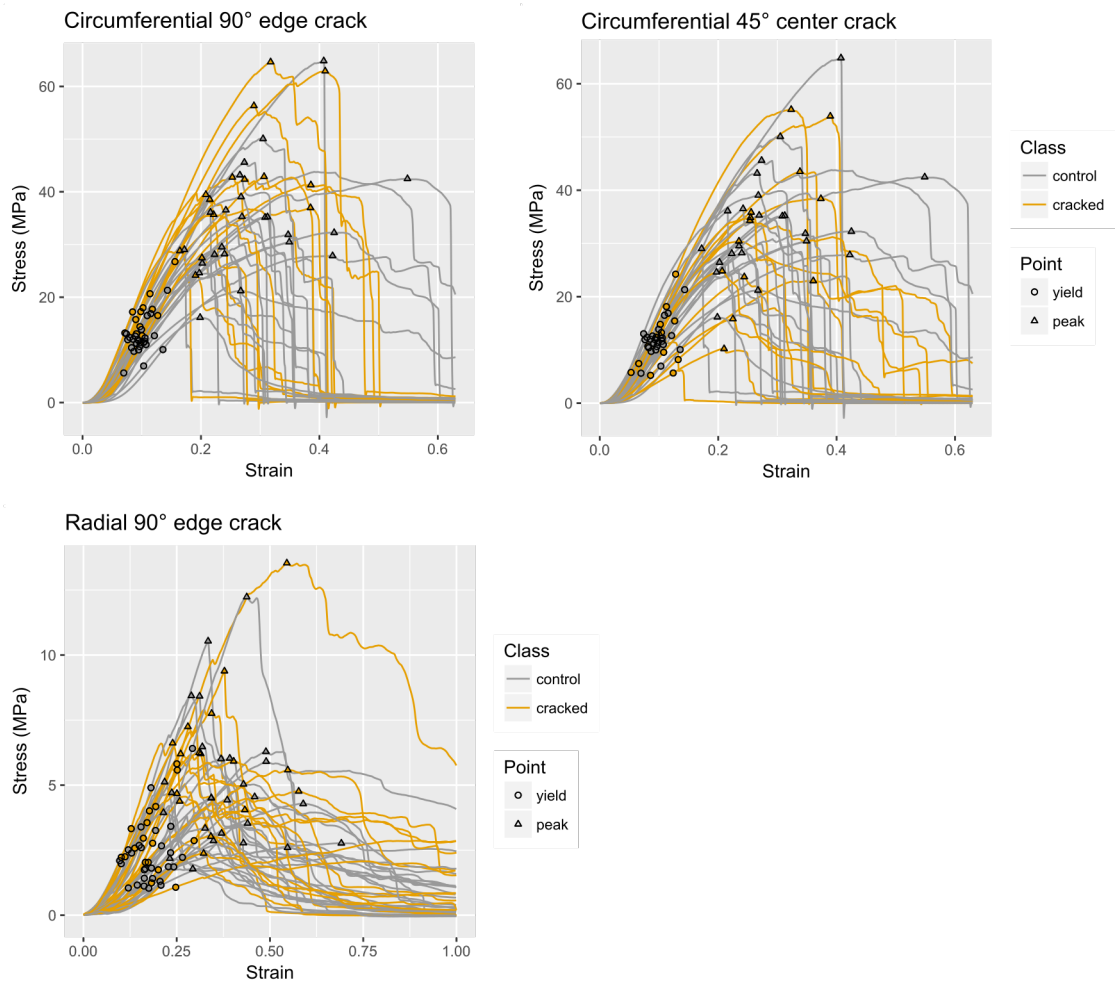

Figure 3: Stress–strain curves for all analyzed specimens.

The other stress–strain curve parameters—peak strain, tangent modulus, yield stress, and yield strain—were also compared between the crack groups and their controls (Figure 2). The full table of stress–strain curve statistics is provided in supplemental information (Table S1), and the stress–strain curves are plotted in Figure 3 for qualitative comparison. Tangent modulus and yield stress were significantly *greater* in circumferential 90° edge crack specimens by 1.5–6.8 MPa and 18–88 MPa respectively (95% CIs). No other stress–strain parameter comparison showed a significant difference between the crack and control groups.

3.2 Effect of cracks on strain fields

The presence of crack-induced strain concentrations was tested by comparing, for each specimen, mean DIC strain near and away from the crack tip. Longitudinal strain (E_{xx}) was significantly greater near the crack tip for all groups at every stress level examined (Figure 4). Transverse strain (E_{yy}) was not significantly different near the crack tip in circumferential tension specimens, but for $\sigma \geq 0.5\sigma_{peak}$ was significantly more compressive near the tip in radial edge crack specimens. Shear strain magnitude ($|E_{xy}|$) was significantly greater near the crack tip in circumferential edge crack specimens for $\sigma \geq 0.8\sigma_{peak}$ and in circumferential center crack and radial edge crack specimens for all stress levels examined. The complete table of strain field statistics is provided in supplemental information (Table S2). These results demonstrate that cracks in meniscus tissue create strain concentrations at their tips.

The strain fields were qualitatively examined in terms of the near-tip strain concentrations' size and shape, as well as the strain fields' overall appearance. Strain fields for three representative cracked specimens are shown in Figure 5. Strain fields for control specimens were similar to those in Peloquin et al. (2016). The mottled appearance of each test's strain field, specifically the pattern of blobs of positive and negative strain, was established early in the test (~ 0.01 strain) and retained the same pattern through failure.

Although the strain fields showed great variation between specimens, they had some consistent features. The near-tip E_{xx} concentrations in circumferential and radial specimens tended to be small and subtle, extending ≈ 0.5 mm from the crack. In radial specimens, the near-tip E_{xx} concentrations sometimes (5/17 tests) grew to extend across the specimen as σ approached σ_{peak} and rupture progressed from the crack tip. Near-tip E_{xy} concentrations in both circumferential and radial specimens took the form of bands that extended longitudinally across 50–100% of the specimen. The crack-associated E_{xy} bands switched sign between sides of the crack. For all strain components, strong strain concentrations tended to develop at multiple places within each specimen. E_{xx} and E_{yy} were on average greater near the crack tip because a strain concentration occurred there consistently across specimens rather than because it was uniquely strong within each specimen. E_{xy}, however, was more sensitive to the presence of a crack; in ~ 1/3 of circumferential tests and ~ 1/2 of radial tests, the strongest and most extensive shear band was crack-associated.

To check that the material cut by the cracks was unloaded, mean strain in the cut region was compared to the intact region (Figure 6; also plotted as an attenuation ratio in Figure S1). Mean E_{xx} in the cut region was significantly less than in the intact region for all crack groups at all stress levels. In edge crack specimens, both circumferential and radial, this effect almost completely abolished E_{xx} in the cut region. Mean E_{yy} in the cut region of radial edge crack specimens was significantly greater than in the intact region, but E_{yy} in

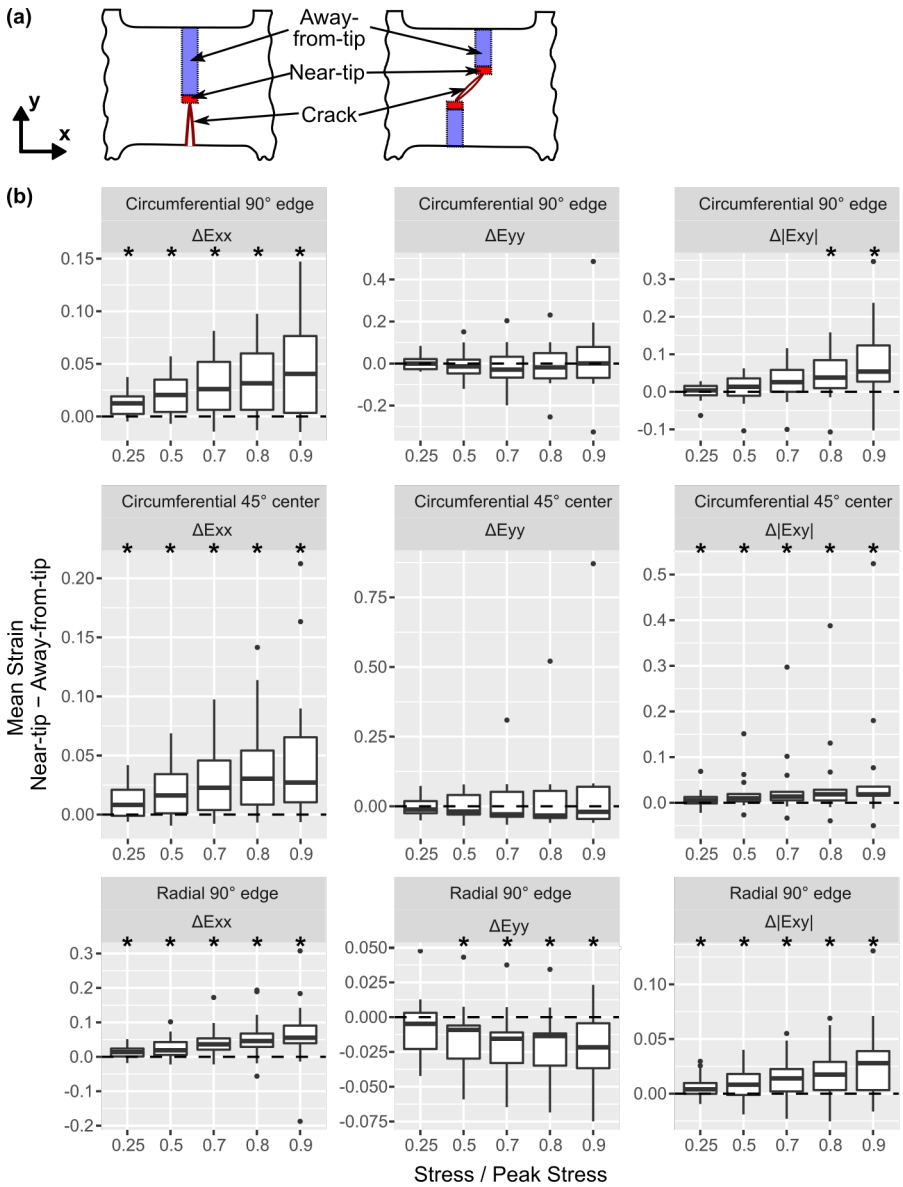

Figure 4: Strain field differences between near-tip and away-from tip regions within specimens. (a) Schematic of region definitions. (b) Tukey boxplots. * near ≠ away, Wilcoxon test, $p < 0.05$.

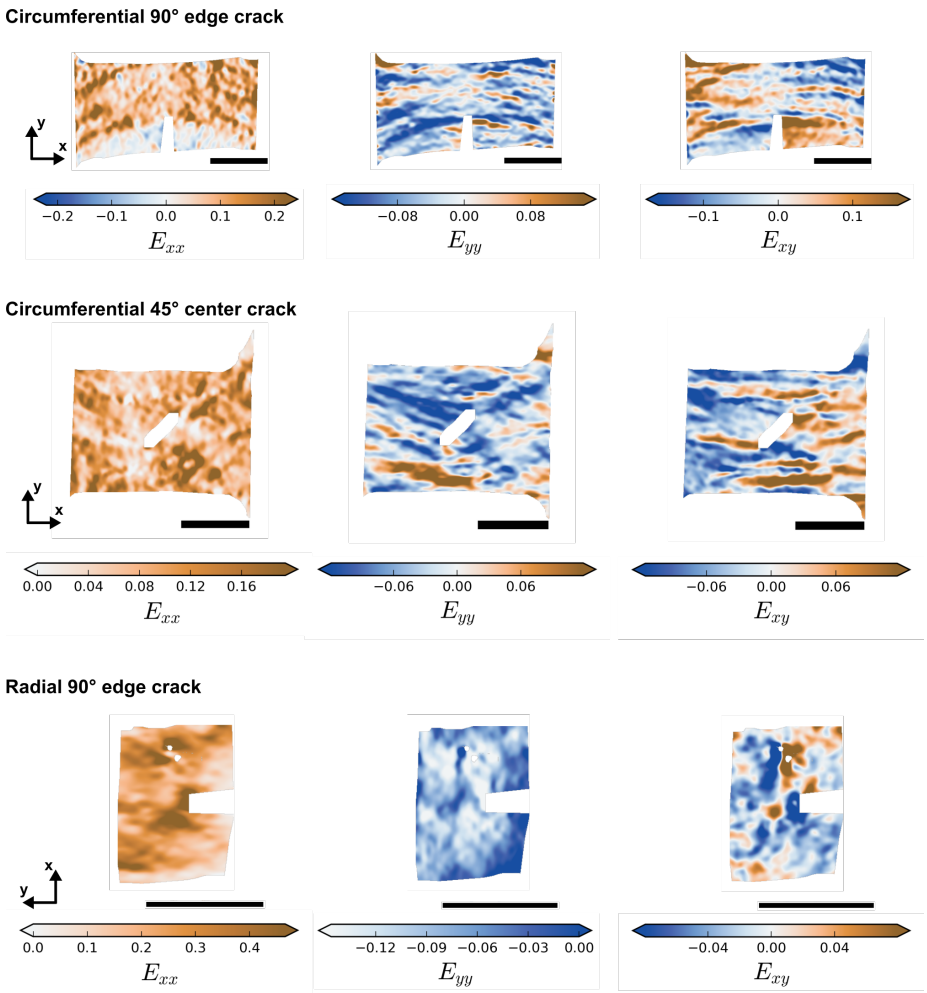

Figure 5: Representative strain fields for cracked specimens in each group at $0.7\sigma_{\mathbf{peak}}$. Scale bar = 5 mm.

the circumferential groups showed no significant effect. Mean $|E_{xy}|$ in the cut region of circumferential edge and center crack specimens was less than in the intact region, whereas in radial edge crack specimens it was greater. As E_{xx} is the strain component most directly related to longitudinal stress, the large reductions in the cut regions' mean E_{xx} values indicate that the crack did unload the cut region.

3.3 Rupture morphology

The visual appearance of the cracked specimens' ruptures is described here to facilitate comparison with other tissues and loading conditions. Rupture in the circumferential edge crack specimens proceeded predominantly by inter-fascicle sliding, creating broad, irregular tears with extensive interdigitating fiber pullout (Figure 7a). In 13 out of 14 circumferential edge crack tests, the region near the crack tip was the first to display visible rupture, but the crack blunted rapidly by inter-fascicle shear (Figure 7b) and final rupture occurred simultaneously over a broad region. Crack blunting by inter-fascicle shear began very early in the test, between $0.2\sigma_{peak}$ and $0.5\sigma_{peak}$. Rupture in circumferential center crack specimens occurred similarly, except that the ruptures at the crack tip were smaller and developed in parallel with separate sites of rupture at the grip line (5 tests) or specimen edge (9 tests). These separate sites of rupture typically joined the crack-associated rupture as they grew (10 tests; Figure 7c). Inter-fascicle shear was ubiquitous in both edge and center crack circumferential specimens, and often caused the rupture line to zigzag across the specimen between zones of interdigitating fiber pullout; a striking example is shown in Figure 7d.

Radial specimens, unlike circumferential specimens, displayed crack extension via incremental, local rupture at the crack tip (Figure 7e). Out of 17 radial tests, 16 had some degree of rupture at the crack tip. In 9 tests, the crack tip-associated rupture grew incrementally and total rupture occurred by crack extension. In 5 of these 9 tests a separate site of rupture developed away from the crack in parallel with the crack extension. Crack tip-associated ruptures did not start until peak stress was approximately reached ($\pm$ 20% peak strain). The 8 radial tests with no sign of crack extension produced rupture at the crack in 3 tests (Figure 7f) and away from it in 5 tests. Regardless of the type of rupture, the rupture site was usually bridged by small fibers (Figures 7e,f). Although in the circumferential specimens the fascicle interfaces appeared to facilitate the formation of shear bands, in the radial specimens they appeared to facilitate incremental crack extension.

The effect of a crack on the type of rupture (midsubstance, mixed, and grip line) was examined by comparing counts of rupture types between cracked specimen groups and their controls (Table 2). Circumferential edge crack specimens had significantly more mixed ruptures, fewer grip line ruptures, and slightly fewer midsubstance ruptures (relative to the total number) than their controls ($p = 0.04$, chi-squared test). Circumferential center crack specimens' rupture type counts were not significantly different from their controls. Radial edge crack specimens had significantly more midsubstance and mixed ruptures and fewer grip line ruptures than their controls ($p = 0.04$, chi-squared test).

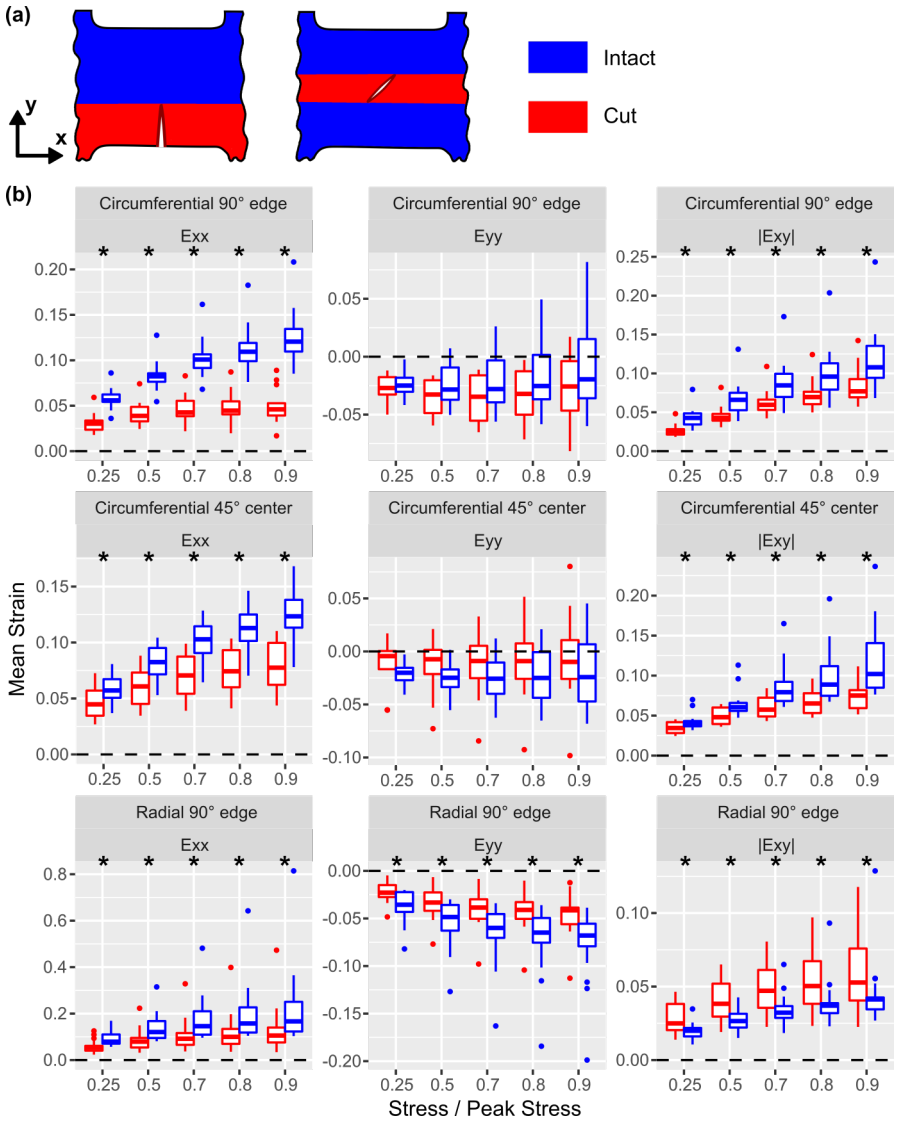

Figure 6: Strain field differences between cut and intact regions within specimens. (a) Region definitions. (b) Tukey boxplots. * indicates cut ≠ intact, paired Wilcoxon test, $p < 0.05$.

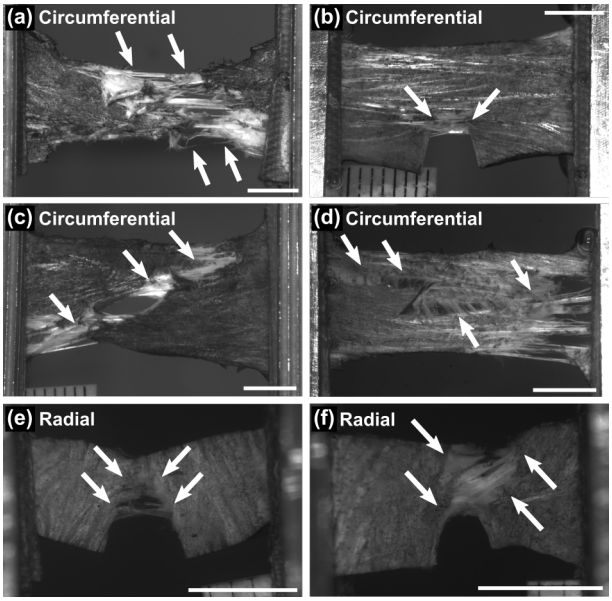

Figure 7: Examples of cracked specimen rupture morphology. (a) Circumferential control, showing the wide rupture zone and interdigitating fiber pullout typical of circumferential specimen bulk rupture. (b) Circumferential edge crack, showing early rupture at the crack tip combined with crack blunting by inter-fascicle shear. (c) Circumferential center crack, showing the typical outcome of independent rupture sites joining the crack. (d) Circumferential center crack, showing zigzagging of a rupture via the crack and the fascicle interfaces. (e) Radial edge crack, showing crack extension. (f) Radial edge crack, showing bulk rupture. (all) Scale bar = 5 mm.

4 Discussion

4.1 Summary of key findings

This study's objective was to determine whether short cracks in meniscus tissue cause failure by fracture and whether they alter the strain field by unloading the cut region and creating a near-tip strain concentration. If failure by fracture occurs, it must do so at stress less than the meniscus' tensile strength; otherwise bulk rupture would occur first. In this study, no reduction in peak stress in cracked specimens was detected relative to controls (Figure 2). Given that the study was powered to detect a meaningful decrease in peak stress, this observed lack of difference in peak stress is a strong indication that fracture did not occur. Regarding strain concentrations, greater tissue strain was observed near the crack tip (Figure 4), implying a corresponding near-tip stress concentration and increased local susceptibility to tissue damage. Consistent with the presence of near-tip strain concentrations, the region cut by the crack had reduced strain, implying unloading (Figure 6). Short meniscus cracks therefore do not cause fracture or otherwise reduce the meniscus' effective strength (peak stress), at least in the conditions tested here, but do create a tip-associated strain & stress concentration with the potential to cause early onset of local tissue damage.

4.2 Significance of lack of fracture

A high degree of resistance to fracture—i.e., toughness—is highly beneficial for meniscus tissue in vivo because the maintenance of strength in the presence of a tear lessens the risk of further failure and loss of function. A tear will still reduce the cross-sectional area and, in proportion, the total force that the meniscus can support. However, the present study's results indicate that short (~ 3 mm) tears in single-cycle loading are unlikely to cause accelerated failure by fracture.

Longer cracks, in principle, produce stronger stress concentrations. In vivo meniscus tears that are considered to definitely require clinical treatment are 5 mm to 25 mm long (Stärke et al. 2009; Roeddecker et al. 1994; Lento and Akuthota 2000; Seil et al. 2009). These tears may exceed the critical length for fracture (Taylor 2007). However, the low risk of fracture for short tears is still beneficial because it should delay the growth of tears to this size. Attempts to replace meniscus tissue with engineered materials should consider replication of the meniscus' toughness as a design requirement.

This assessment of low risk for short meniscus tears has caveats, as the excised tissue test conditions were, by necessity, artificial. Specimen size and hence crack length was small, only edge and center cracks were examined, specimens were cut only from the center of the meniscus, specimens were loaded only in circumferential and radial uniaxial tension, cutting specimens may cause loss of fiber integrity, the loading rate was relatively slow (0.5 mm/s), and the tensile grips work by compression and friction rather than by individually anchoring each fiber like the enthesis. In vivo, tears come in a wide variety of geometries and the meniscus is subjected to surface contact and multiaxial, heterogeneous stress (Kawamura et al. 2003; Fithian et al. 1990; Mononen et al. 2013; Aspden 1985; Spilker et al. 1992; Párraga Quiroga et al. 2014; Atmaca et al. 2013; Freutel et al. 2014). Considerable work remains to, in laboratory tests, reproduce the wide variety of loading conditions under which the meniscus must function in vivo and to quantify damage and failure in those

conditions. Pending development of more advanced methods, however, the present results support a low risk of total failure due to short tears.

4.3 Significance of crack tip strain concentrations

Although cracks did not decrease the meniscus specimens' effective strength, they did create regions of greater strain near their tips. These strain concentrations were substantial. Depending on the test scenario and stress level, mean longitudinal strain was increased by 20% to 50% and mean shear strain magnitude was increased by 20% to 80% (Figure 4). Groups with more complete unloading of the cut region (circumferential and radial edge crack specimens) also had greater E_{xx} concentrations, consistent with load redistribution around the crack being the cause of the strain concentrations. This near-tip overstrain has potential to cause local damage and failure under normal load levels. Damage is generally reported to begin at 0.05–0.08 strain in tendon and ligament (Provenzano et al. 2002; Duenwald-Kuehl et al. 2012; Sverdlik and Lanir 2002; Zitnay et al. 2017), with one study showing a damage threshold ≈ 0.02 strain (Lee et al. 2017), but thresholds for damage or permanent deformation are not known for meniscus. If the meniscus is similar to tendon and ligament, the stress threshold at which a crack makes meniscus tissue vulnerable to damage would be 25–50% of its tensile strength; that is, 9–17 MPa. At these stress levels, crack blunting via inter-fascicle shear was prevalent in circumferential edge and center crack specimens and rupture from the crack tip along fascicle boundaries was prevalent in circumferential edge crack specimens. These phenomena indicate that the near-tip shear concentrations promoted the rupture of inter-fascicle connections. Furthermore, the existence of zones of weakness near the tips of natural meniscus tears suggests that damage due to strain concentrations also occurs in vivo (Roeddecker et al. 1994). Local strain concentrations created by cracks in meniscus tissue therefore pose a high risk of causing local damage.

4.4 Combined interpretation of lack of fracture and strain concentrations

The apparent low risk of fracture and total failure in meniscus tissue with a crack stands in contrast to the high risk of local damage near the crack tip. These risks may have an inherent trade-off. Toughness represents the energy required for crack growth. Local energy dissipation around the crack tip, such as by plastic zone phenomena, increases toughness (Taylor et al. 2012; Janssen et al. 2002). The observed near-tip zone of local overstrain and probable damage may function as a dissipative zone, with the function of increasing toughness and limiting crack growth. Inter-fascicle shear, which was especially strong in circumferential specimens, may increase the meniscus' toughness by absorbing energy through fascicle sliding. Inter-fascicle sliding also acts to deflect the path of rupture along fascicle boundaries (e.g., Figure 7d), which due to the circumferential specimens' geometry promotes rupture by processes other than crack opening and extension. In radial specimens, the parallel alignment of the fascicles and the crack prevented fascicle sliding from acting as a crack deflection mechanism, which is likely why half of radial specimens exhibited crack extension (albeit still without significant fracture). The roles of local damage, plasticity,

and crack deflection as toughening mechanisms in the meniscus warrant further investigation.

Strain concentrations near the tip of a meniscus tear, when subjected to long-term repeated loading, may cause accumulation of incremental damage and failure. In circumferential tests, shear strain concentrations extended 5–10 mm from the crack tip, along fascicle boundaries, and were halted by the grip line. In vivo they would not be restricted in this manner and hence could provide a pathway for progressive growth of circumferential, bucket handle, vertical, and/or horizontal tears (Aspden 1985; Fithian et al. 1990; Kelly et al. 1990; Smillie 1978). A strain concentration may also kill or damage cells, even in a single loading cycle. In ligament, cell death has been shown to follow a linear no-threshold model with applied strain (Provenzano et al. 2002). A meniscus tear should also cause regional unloading similar to that observed here for cracks (Figure 6), which may lead to pathology due to cells' dependence on load to maintain homeostasis (Natsu-Ume et al. 2005; Frank et al. 2004; Gupta et al. 2008). Altered cell loading and cumulative tissue and cell damage may mediate long-term development of in vivo meniscus pathology.

4.5 Increased tangent modulus and yield stress in edge crack circumferential tests

The observation of greater tangent modulus and yield stress in edge crack circumferential tests compared to controls (Figure 2) was unexpected and its cause is indeterminate. One possibility is that it occurred by chance; i.e., that it is a type I statistical error. A second possibility is that the inner margin of a circumferential specimen has an effective stiffness less than the outer margin. If so, the edge crack, by eliminating the low-stiffness inner margin from the intact cross-section, would cause the average modulus to increase. A lesser effective stiffness in the inner margin implies that the peak stress for circumferential edge crack specimens should have also increased; this is neither confirmed nor ruled out by the data ($p = 0.07$, post-hoc two-tailed t-test). A lesser effective stiffness in the inner margin of circumferential specimens, if present, could have been caused by differences between the inner and outer margins in either (a) material properties or (b) fascicle loading.

The meniscus' material properties, specifically tissue composition and stiffness, have been observed to vary with radial position in the meniscus (Cheung 1987; Kelly et al. 1990; Nakano et al. 1986; Ghosh et al. 1983; Fithian et al. 1990). However, these comparisons were of the outer, central, and inner thirds, and the specimens in the present study were all cut from the central third. Electron microscopy and histology show homogeneous composition in the central third (Petersen and Tillmann 1998; Andrews et al. 2014). There is no prior evidence that the inner margin of specimens in the present study should have significantly different material properties from the rest of the specimen. The observation of greater tangent modulus and yield stress in edge crack circumferential specimens is therefore unlikely to have been caused by radial position-dependent differences in material properties.

A reduction in fascicle loading within the inner margin of circumferential specimens could have been caused by the specimens' geometry. The meniscus' fascicles are aligned in arcs, but the specimens' edges were straight. A portion of the inner margin's fascicles were therefore discontinuous with the gripped region and were loaded indirectly by inter-fascicle shear. The fascicle interfaces are compliant and shear readily (Figures 5 and 7b), so load transfer to the discontinuous fascicles is likely to be slight. This effect has been quantified

in annulus fibrosus and tendon (Skaggs et al. 1994; Szczesny et al. 2015). The inner margin's fascicles may therefore be relatively unloaded, contributing little to the stiffness of the specimen. Unloaded inner margin fascicles would artificially decrease the average modulus in circumferential control and center crack specimens, which have an intact inner edge, but not in edge crack specimens because the crack eliminates these inner margin fascicles from the load-bearing cross-sectional area.

The potential for fascicle unloading due to the mismatch between straight sides of conventional tensile test specimens and their arced fascicle geometry deserves further investigation. Interactions between specimen geometry and fiber continuity have been previously shown to alter the meniscus' apparent tensile properties (Peloquin et al. 2016), prompting the use of expanded grip regions. However, the present tangent modulus and yield stress results suggest that the meniscus' arced fascicle architecture may remain a challenge. In vivo, the meniscus' entheses likely provide much more effective fiber loading than is currently possible in laboratory tests.

4.6 In vivo tear growth and future directions

The general lack of crack extension observed in this study leaves the mechanisms by which meniscus tears grow in vivo uncertain. In particular, it would be very useful to know the time period for which a short meniscus tear can be expected to remain short and hence low-risk in vivo. High cycle loading, as has recently been undertaken for crack-free meniscus (Creechley et al. 2017), is a promising approach. Loading rate is another potentially important factor. Meniscus tears often occur in the context of sports, implying involvement of high-rate loading (Drosos and Pozo 2004; Feucht et al. 2015), and ex vivo impact testing has produced meniscus tears (Isaac et al. 2010; Isaac et al. 2008). It is possible that a high-rate loading cycle (as would be expected from an impact) can produce a long (5–25 mm) tear of clinical concern immediately, without slow growth from a low-risk short tear. The central task for future experiments is to produce physiologic growth of cracks under controlled laboratory conditions so that the mechanisms and time course of this pathology can be quantified.

5 Acknowledgments

Research reported in this publication was supported by NIAMS of the National Institutes of Health under award numbers R01 AR050052 and R21 AR070966. Additional support was provided by a Delaware CTR ACCEL ShoRE PGP grant under NIH U54 GM104941. The content is solely the responsibility of the authors and does not necessarily represent the official views of the National Institutes of Health. Julia Pezick and Pranita Muralidhar contributed a great deal to this work by performing many of the mechanical tests.

6 Supporting information captions

Figure S1. Ratios between mean strain in cut and intact regions. The plots of E_{yy} ratios for the circumferential edge and center crack groups are cropped to exclude 3 specimens

each for which intact strain ≈ 0. All plotted quantiles, however, are based on the full dataset. The boxplots are in Tukey's style.

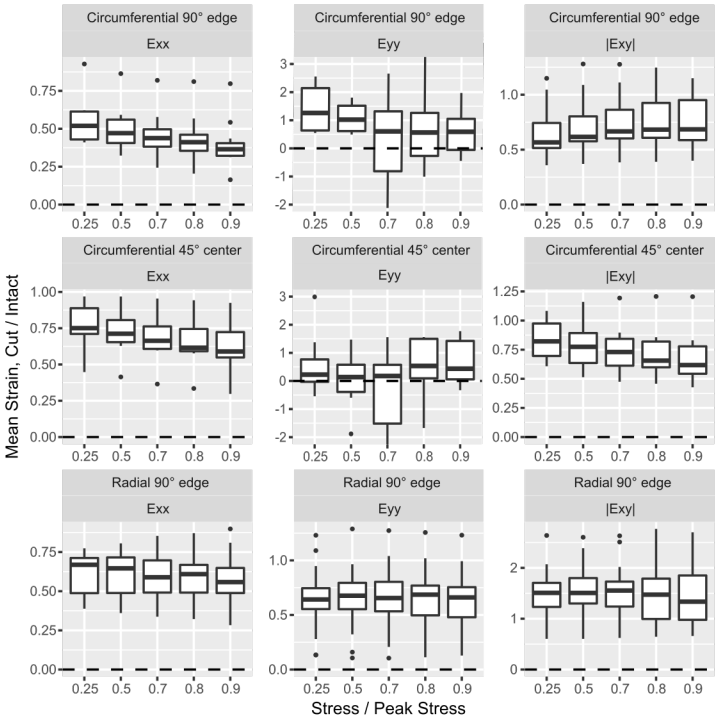

Table S1. Complete stress–strain curve statistics for all groups. See supplemental files.

Table S2. Complete strain field statistics by region for cracked groups. See supplemental files.

References

Andarawis-Puri, Nelly, Eric T. Ricchetti, and Louis J. Soslowsky (2009). "Rotator cuff tendon strain correlates with tear propagation". In: *Journal of Biomechanics* 42.2, pp. 158–163.

Andrews, Stephen H. J., Jerome B. Rattner, Ziad Abusara, Adetola Adesida, Nigel G. Shrive, and Janet L. Ronsky (2014). "Tie-fibre structure and organization in the knee menisci". In: *Journal of Anatomy* 224.5, pp. 531–537.

Anetzberger, Hermann, Alexandra Mayer, Christian Glaser, Stephan Lorenz, Christof Birkenmaier, and Magdalena Müller-Gerbl (2014). "Meniscectomy leads to early changes in the mineralization distribution of subchondral bone plate". In: *Knee Surgery, Sports Traumatology, Arthroscopy* 22.1, pp. 112–119.

Arnoczky, S. P. and R. F. Warren (1983). “The microvasculature of the meniscus and its response to injury. An experimental study in the dog”. In: *The American Journal of Sports Medicine* 11.3, pp. 131–141.

Aspden, R. M. (1985). “A model for the function and failure of the meniscus”. In: *Engineering in Medicine* 14.3, pp. 119–122.

Atmaca, Halil, Cevdet Cumhur Kesemenli, Kaya Memişoğlu, Arif Özkan, and Yusuf Celik (2013). “Changes in the loading of tibial articular cartilage following medial meniscectomy: a finite element analysis study”. In: *Knee Surgery, Sports Traumatology, Arthroscopy* 21.12, pp. 2667–2673.

Cheung, H. S. (1987). “Distribution of type I, II, III and V in the pepsin solubilized collagens in bovine menisci”. In: *Connective Tissue Research* 16.4, pp. 343–356.

Chin-Purcell, Michele V. and Jack L. Lewis (1996). “Fracture of articular cartilage”. In: *Journal of Biomechanical Engineering* 118.4, p. 545.

Cohen, Moises, Joicemar Tarouco Amaro, Benno Ejnisman, Rogério Teixeira Carvalho, Kleber Kodi Nakano, Maria Stella Peccin, Rogério Teixeira, Cristiano F. S. Laurino, and Rene Jorge Abdalla (2007). “Anterior cruciate ligament reconstruction after 10 to 15 years: association between meniscectomy and osteoarthrosis”. In: *Arthroscopy* 23.6, pp. 629–634.

Cox, Charles L., Joseph P. Deangelis, Robert A. Magnussen, R. Warne Fitch, and Kurt P. Spindler (2009). “Meniscal tears in athletes”. In: *Journal of Surgical Orthopaedic Advances* 18.1, pp. 2–8.

Creechley, Jaremy J., Madison E. Krentz, and Trevor J. Lujan (2017). “Fatigue life of bovine meniscus under longitudinal and transverse tensile loading”. In: *Journal of the Mechanical Behavior of Biomedical Materials* 69, pp. 185–192.

Drosos, G. I. and J. L. Pozo (2004). “The causes and mechanisms of meniscal injuries in the sporting and non-sporting environment in an unselected population”. In: *The Knee* 11.2, pp. 143–149.

Duenwald-Kuehl, Sarah, Jaclyn Kondratko, Roderic S. Lakes, and Ray Vanderby Jr (2012). “Damage mechanics of porcine flexor tendon: mechanical evaluation and modeling”. In: *Annals of Biomedical Engineering* 40.8, pp. 1692–1707.

Englund, Martin, Ali Guermazi, Daniel Gale, David J. Hunter, Piran Aliabadi, Margaret Clancy, and David T. Felson (2008). “Incidental meniscal findings on knee MRI in middle-aged and elderly persons”. In: *The New England Journal of Medicine* 359.11, pp. 1108–1115.

Englund, Martin, Frank W. Roemer, Daichi Hayashi, Michel D. Crema, and Ali Guermazi (2012). “Meniscus pathology, osteoarthritis and the treatment controversy”. In: *Nature Reviews Rheumatology* 8.7, pp. 412–419.

Favata, Michele (2006). “Scarless healing in the fetus: Implications and strategies for postnatal tendon repair”. PhD thesis. University of Pennsylvania.

Feucht, Matthias J., Sebastian Bigdon, Gerrit Bode, Gian M. Salzmann, David Dovi-Akue, Norbert P. Südkamp, and Philipp Niemeyer (2015). “Associated tears of the lateral meniscus in anterior cruciate ligament injuries: risk factors for different tear patterns”. In: *Journal of Orthopaedic Surgery and Research* 10.34.

Fink, Kyle, Neil Kaushal, Jordan Gross, Himanshu Patel, and Damon Delbello (2018). “Bucket-handle tear of the medial meniscus in a 2-year-old child”. In: *Orthopedics*, pp. 1–3.

Fithian, D. C., M. A. Kelly, and V. C. Mow (1990). "Material properties and structure-function relationships in the menisci". In: *Clinical Orthopaedics and Related Research* 252, pp. 19–31.

Frank, C. B., N. G. Shrive, R. S. Boorman, I. K. Y. Lo, and D. A. Hart (2004). "New perspectives on bioengineering of joint tissues: joint adaptation creates a moving target for engineering replacement tissues". In: *Annals of Biomedical Engineering* 32.3, pp. 458–465.

Freutel, Maren, Andreas M. Seitz, Fabio Galbusera, Axel Bornstedt, Volker Rasche, Melissa L. Knothe Tate, Anita Ignatius, and Lutz Dürselen (2014). "Medial meniscal displacement and strain in three dimensions under compressive loads: MR assessment". In: *Journal of Magnetic Resonance Imaging* 40.5, pp. 1181–1188.

Ghosh, P., T. K. Taylor, G. D. Pettit, B. A. Horsburgh, and C. R. Bellenger (1983). "Effect of postoperative immobilisation on the regrowth of the knee joint semilunar cartilage: an experimental study". In: *Journal of Orthopaedic Research* 1.2, pp. 153–164.

Greis, Patrick E., Davide D. Bardana, Michael C. Holmstrom, and Robert T. Burks (2002). "Meniscal Injury: I. Basic Science and Evaluation". In: *Journal of the American Academy of Orthopaedic Surgeons* 10.3, pp. 168–176.

Gupta, T., B. Zielinska, J. McHenry, M. Kadmiel, and T. L. Haut Donahue (2008). "IL-1 and iNOS gene expression and NO synthesis in the superior region of meniscal explants are dependent on the magnitude of compressive strains". In: *Osteoarthritis and Cartilage* 16.10, pp. 1213–1219.

Hardin, G. T., J. Farr, and B. R. Bach (1992). "Meniscal tears: diagnosis, evaluation, and treatment". In: *Orthopaedic Review* 21.11, pp. 1311–1317.

Isaac, Daniel I., Eric G. Meyer, and Roger C. Haut (2008). "Chondrocyte damage and contact pressures following impact on the rabbit tibiofemoral joint". In: *Journal of Biomechanical Engineering* 130.4, p. 041018.

— (2010). "Development of a traumatic anterior cruciate ligament and meniscal rupture model with a pilot in vivo study". In: *Journal of Biomechanical Engineering* 132.6, p. 064501.

Janssen, M., J. Zuidema, and R. J. H. Wanhill (2002). *Fracture Mechanics*. 2nd ed. Delft, The Netherlands: VSSD.

Kawamura, Sumito, Kristin Lotito, and Scott A. Rodeo (2003). "Biomechanics and healing response of the meniscus". In: *Operative Techniques in Sports Medicine* 11.2, pp. 68–76.

Kelly, M. A., D. C. Fithian, K. Y. Chern, and V. C. Mow (1990). "Structure and function of the meniscus: basic and clinical implications". In: *Biomechanics of Diarthrodial Joints*. Ed. by Anthony Ratcliffe, Savio L.-Y. Woo, and Van C. Mow. Springer New York, pp. 191–211.

Khan, Hussain Ijaz, Dawn Aitken, Changhai Ding, Leigh Blizzard, Jean-Pierre Pelletier, Johanne Martel-Pelletier, Flavia Cicuttini, and Graeme Jones (2016). "Natural history and clinical significance of meniscal tears over 8 years in a midlife cohort". In: *BMC Musculoskeletal Disorders* 17, p. 4.

Koombua, Kittisak, Ramana M. Pidaparti, and Mark W. Beatty (2006). "Fracture toughness estimation for the TMJ disc". In: *Journal of Biomedical Materials Research Part A* 79.3, pp. 566–573.

Kumm, Jaanika, Frank W. Roemer, Ali Guermazi, Aleksandra Turkiewicz, and Martin Englund (2015). "Natural history of intrameniscal signal intensity on knee MR images: six years of data from the Osteoarthritis Initiative". In: *Radiology* 278.1, pp. 164–171.

Lee, Andrea H., Spencer E. Szczesny, Michael H. Santare, and Dawn M. Elliott (2017). "Investigating mechanisms of tendon damage by measuring multi-scale recovery following tensile loading". In: *Acta Biomaterialia*.

Lento, P. H. and V. Akuthota (2000). "Meniscal injuries: a critical review". In: *Journal of Back and Musculoskeletal Rehabilitation* 15.2, pp. 55–62.

Locke, Ryan C., John M. Peloquin, Elisabeth A. Lemmon, Adrianna Szostek, Dawn M. Elliott, and Megan L. Killian (2017). "Strain distribution of intact rat rotator cuff tendon-to-bone attachments and attachments with defects". In: *Journal of Biomechanical Engineering* 139.11.

Magnussen, Robert A., Alfred A. Mansour, James L. Carey, and Kurt P. Spindler (2009). "Meniscus status at anterior cruciate ligament reconstruction associated with radiographic signs of osteoarthritis at 5- to 10-year follow-up: a systematic review". In: *The Journal of Knee Surgery* 22.4, pp. 347–357.

Mononen, Mika E., Jukka S. Jurvelin, and Rami K. Korhonen (2013). "Effects of radial tears and partial meniscectomy of lateral meniscus on the knee joint mechanics during the stance phase of the gait cycle—A 3D finite element study". In: *Journal of Orthopaedic Research* 31.8, pp. 1208–1217.

Nakano, T., J. R. Thompson, and F. X. Aherne (1986). "Distribution of glycosaminoglycans and the nonreducible collagen crosslink, pyridinoline in porcine menisci". In: *Canadian Journal of Veterinary Research* 50.4, pp. 532–536.

Natsu-Ume, Takashi, Tokifumi Majima, Carol Reno, Nigel G. Shrive, Cyril B. Frank, and David A. Hart (2005). "Menisci of the rabbit knee require mechanical loading to maintain homeostasis: cyclic hydrostatic compression in vitro prevents derepression of catabolic genes". In: *Journal of Orthopaedic Science* 10.4, pp. 396–405.

Oberlander, M. A. and J. A. Pryde (1994). "Meniscal injuries". In: *The Hughston Clinic Sports Medicine Book*. Ed. by C. L. Baker. Media, PA: Williams and Wilkins, pp. 465–472.

Øiestad, Britt Elin, Lars Engebretsen, Kjersti Storheim, and May Arna Risberg (2009). "Knee osteoarthritis after anterior cruciate ligament injury: a systematic review". In: *The American Journal of Sports Medicine* 37.7, pp. 1434–1443.

Párraga Quiroga, J. M., P. Emans, W. Wilson, K. Ito, and C. C. van Donkelaar (2014). "Should a native depth-dependent distribution of human meniscus constitutive components be considered in FEA-models of the knee joint?" In: *Journal of the Mechanical Behavior of Biomedical Materials* 38, pp. 242–250.

Paul, Jonathan J., Kurt P. Spindler, Jack T. Andrish, Richard D. Parker, Michelle Secic, and John A. Bergfeld (2003). "Jumping versus nonjumping anterior cruciate ligament injuries: a comparison of pathology". In: *Clinical Journal of Sport Medicine* 13.1, pp. 1–5.

Peloquin, John M. and Dawn M. Elliott (2016). "A comparison of stress in cracked fibrous tissue specimens with varied crack location, loading, and orientation using finite element analysis". In: *Journal of the Mechanical Behavior of Biomedical Materials* 57, pp. 260–268.

Peloquin, John M., Michael H. Santare, and Dawn M. Elliott (2016). “Advances in quantification of meniscus tensile mechanics including nonlinearity, yield, and failure”. In: *Journal of Biomechanical Engineering* 138.2, p. 021002.

Petersen, W. and B. Tillmann (1998). “Collagenous fibril texture of the human knee joint menisci”. In: *Anatomy and Embryology* 197.4, pp. 317–324.

Petty, Catherine A. and James H. Lubowitz (2011). “Does arthroscopic partial meniscectomy result in knee osteoarthritis? A systematic review with a minimum of 8 years’ follow-up”. In: *Arthroscopy* 27.3, pp. 419–424.

Poulsen, Matthew R. and Darren L. Johnson (2011). “Meniscal injuries in the young, athletically active patient”. In: *The Physician and Sportsmedicine* 39.1, pp. 123–130.

Provenzano, Paolo P., Dennis Heisey, Kei Hayashi, Roderic Lakes, and Ray Vanderby Jr (2002). “Subfailure damage in ligament: a structural and cellular evaluation”. In: *Journal of Applied Physiology* 92.1, pp. 362–371.

Roeddecker, K., U. Muennich, and M. Nagelschmidt (1994). “Meniscal healing: a biomechanical study”. In: *Journal of Surgical Research* 56.1, pp. 20–27.

Schechtman, H. and D. L. Bader (1997). “In vitro fatigue of human tendons”. In: *Journal of Biomechanics* 30.8, pp. 829–835.

Seil, R., N. VanGiffen, and D. Pape (2009). “Thirty years of arthroscopic meniscal suture: What’s left to be done?” In: *Orthopaedics & Traumatology, Surgery & Research* 95.8 Suppl 1, S85–96.

Shelbourne, K. D. and T. Gray (2000). “Results of anterior cruciate ligament reconstruction based on meniscus and articular cartilage status at the time of surgery. Five- to fifteen-year evaluations”. In: *The American Journal of Sports Medicine* 28.4, pp. 446–452.

Skaggs, D. L., M. Weidenbaum, James C. Iatridis, A. Ratcliffe, and Van C. Mow (1994). “Regional variation in tensile properties and biochemical composition of the human lumbar anulus fibrosus”. In: *Spine* 19.12, pp. 1310–1319.

Smillie, Ian Scott (1978). *Injuries of the Knee Joint*. Edinburgh; New York; New York: Churchill Livingstone ; Distributed by Longman.

Spilker, R. L., P. S. Donzelli, and Van C. Mow (1992). “A transversely isotropic biphasic finite element model of the meniscus”. In: *Journal of Biomechanics* 25.9, pp. 1027–1045.

Stärke, Christian, Sebastian Kopf, Wolf Petersen, and Roland Becker (2009). “Meniscal repair”. In: *Arthroscopy* 25.9, pp. 1033–1044.

Sverdlik, A. and Y. Lanir (2002). “Time-dependent mechanical behavior of sheep digital tendons, including the effects of preconditioning”. In: *Journal of Biomechanical Engineering* 124.1, pp. 78–84.

Szczesny, Spencer E., Jeffrey L. Caplan, Pal Pedersen, and Dawn M. Elliott (2015). “Quantification of Interfibrillar Shear Stress in Aligned Soft Collagenous Tissues via Notch Tension Testing”. In: *Scientific Reports* 5, p. 14649.

Szczesny, Spencer E., John M. Peloquin, Daniel H. Cortes, Jennifer A. Kadlowec, Louis J. Soslowsky, and Dawn M. Elliott (2012). “Biaxial tensile testing and constitutive modeling of human supraspinatus tendon”. In: *Journal of Biomechanical Engineering* 134.2, p. 021004.

Taylor, David (2007). *The Theory of Critical Distances: A New Perspective in Fracture Mechanics*. 1st ed. Elsevier Science.

Taylor, David, Niamh O'Mara, Eoin Ryan, Michael Takaza, and Ciaran Simms (2012). "The fracture toughness of soft tissues". In: *Journal of the Mechanical Behavior of Biomedical Materials* 6, pp. 139–147.

Von Forell, Gregory A. and Anton E. Bowden (2014a). "A damage model for the percutaneous triple hemisection technique for tendo-achilles lengthening". In: *Journal of Biomechanics*.

— (2014b). "Biomechanical implications of lumbar spinal ligament transection". In: *Computer Methods in Biomechanics and Biomedical Engineering* 17.15, pp. 1685–1695.

Wagemakers, Harry P. A., Edith M. Heintjes, Simone S. Boks, Marjolein Y. Berger, Jan A. N. Verhaar, Bart W. Koes, and Sita M. A. Bierma-Zeinstra (2008). "Diagnostic value of history-taking and physical examination for assessing meniscal tears of the knee in general practice". In: *Clinical Journal of Sport Medicine* 18.1, pp. 24–30.

Zitnay, Jared L., Yang Li, Zhao Qin, Boi Hoa San, Baptiste Depalle, Shawn P. Reese, Markus J. Buehler, S. Michael Yu, and Jeffrey A. Weiss (2017). "Molecular level detection and localization of mechanical damage in collagen enabled by collagen hybridizing peptides". In: *Nature Communications* 8, p. 14913.